Modeling of Coplanar Stripline Discontinuities

Rainee N. Simons, *Senior Member, IEEE*, Nihad I. Dib, *Member, IEEE*, and Linda P. B. Katehi, *Fellow, IEEE*

***Abstract*— The paper presents a technique to obtain lumped equivalent circuit models for typical coplanar stripline (CPS) discontinuities such as an open circuit, a short circuit, and a series gap in one of the strip conductors and gives their element values as a function of the discontinuity physical dimensions for a specific substrate. The model element values are determined from the discontinuity scattering parameters which are de-embedded from the measured scattering parameters using a thru-reflect-line (TRL) algorithm. In addition, the resonant frequency of a spur-slot is presented as a function of the spur length. The experimental results are validated by data obtained using the finite-difference time-domain (FDTD) technique.**

I. Introduction

A coplanar stripline (CPS) [1] on a dielectric substrate of thickness D consists of a pair of strip conductors of width W and separated by a narrow slot of width S, as shown in Fig. 1. In this transmission line, the electric field lines extend across the slot and the magnetic field lines encircle the strip conductors. In the past, the microstrip line and the coplanar waveguide (CPW) were the two preferred transmission media for realizing microwave integrated circuits (MIC's). Other transmission media such as slot line and CPS were perceived to have excess loss and transitions to microstrip and CPW in real applications were considered to be too complex. However with the advent of uniplanar circuits and CPW with finite ground planes this perception has changed. The CPS has several advantages over conventional microstrip line: it facilitates easy shunt as well as series mounting of active and passive devices and it eliminates the need for wraparound and via holes which introduce additional parasitic elements [2], [3]. The CPS has all the advantages of coplanar waveguide (CPW) which is the dual structure and in addition, the CPS makes efficient use of the wafer area and thus the die size per circuit function is small. This results in lower cost and larger number of circuit functions for a given die size. Also, the CPS propagation parameters are independent of the substrate thickness beyond a certain critical thickness which simplifies heat sinking and circuit packaging. Previous applications of CPS includes feed network for printed dipoles and linearly tapered slot antennas for which a transition from CPW to CPS [4] and from microstrip to CPS [5], respectively, have been fabricated and characterized.

Manuscript received August 22, 1995; revised January 17, 1996.

R. N. Simons is with NASA Lewis Research Center, Nyma Group, Cleveland, OH 44135 USA.

N. I. Dib was with the University of Michigan and is now with the Electrical Engineering Department, Jordan University of Science and Technology, Irbid, Jordan.

L. P. B. Katehi is with the Radiation Laboratory 3240, Electrical Engineering and Computer Sciences Department, University of Michigan, Ann Arbor, MI 48109-2122 USA.

Publisher Item Identifier S 0018-9480(96)03025-6.

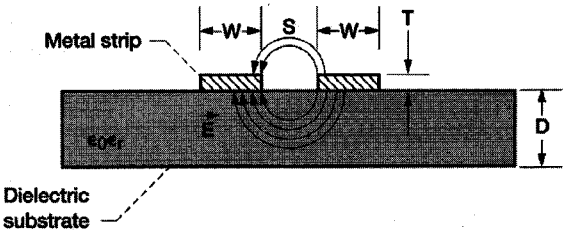

Fig. 1. Cross section of the coplanar stripline. $D = 0.03$ in, $\epsilon_r = 10.2$, $T = 0.00067$ in.

In the past, lumped-element equivalent circuit models for discontinuities in planar microwave transmission media, such as, microstrip and CPW have been obtained using resonator [6] and two-tier de-embedding [7] techniques, respectively. This paper presents for the first time a technique to obtain lumped-element equivalent circuit models for typical CPS discontinuities together with element values as a function of the discontinuity physical dimensions for a specific substrate. These element values are determined from the discontinuity scattering parameters (S-parameters) which are de-embedded from the measured S-parameters using a thru-reflect-line (TRL) algorithm. The discontinuities characterized in this paper are an abrupt open circuit, an open circuit with an extended strip conductor, a short circuit, a series gap in one of the strip conductors, and a spur-slot. These CPS discontinuities are fabricated on a 0.03 in thick RT-Duroid 6010 substrate ($\epsilon_r = 10.2$) with 0.5 oz. copper cladding. These discontinuities are characterized over the frequency range of 2 to 12 GHz. For validation purposes, the experimental results are compared to data obtained using the finite-difference time-domain (FDTD) method [8]. Although, the results presented in the paper are for a specific substrate, the measurement technique as well as the numerical simulation method are quite general and can easily be extended to other substrate materials and higher frequencies. The CPS has potential applications in the design of microwave components such as filters, couplers, mixers, oscillators, and amplifiers for the emerging wireless communications.

II. Theoretical and Experimental Characterization Techniques for CPS Discontinuities

A. Theory

The application of the FDTD technique to planar transmission lines has been described extensively in the literature [9]–[11]. In this method, Maxwell's curl equations are expressed in discretized space and time domains and are then used to simulate the propagation of an initial excita-

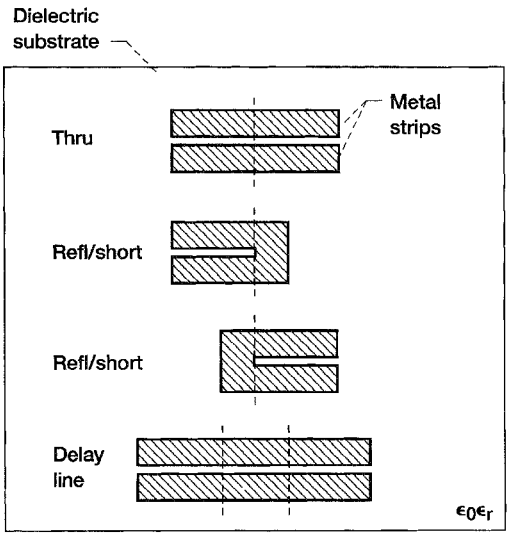

Fig. 2. Schematic of CPS thru-reflect-line (TRL) on-wafer calibration standards.

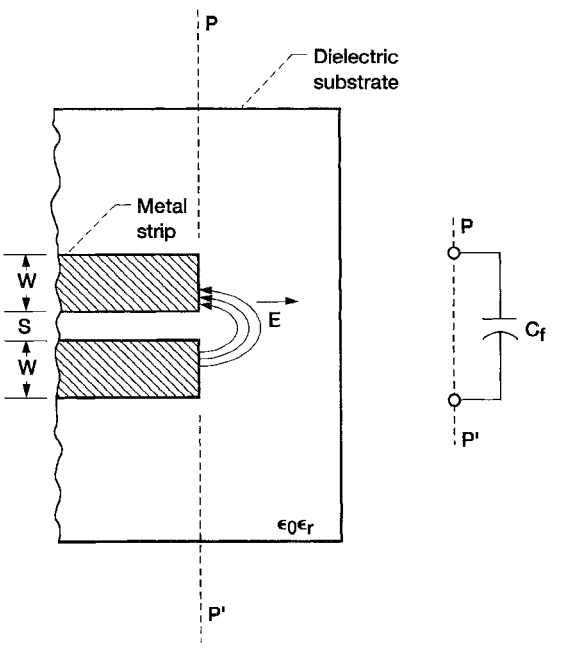

Fig. 3. Coplanar stripline open circuit and a lumped capacitance equivalent circuit model.

tion in a "leapfrog" manner. In order to characterize any planar discontinuity, propagation of a specific time-dependent function, usually a Gaussian pulse, through the structure is simulated using the FDTD technique. A Gaussian pulse is used here because it is smoothly varying in time, and its Fourier transform is also a Gaussian function centered at zero frequency. Following the time and space discretizations of the electric and magnetic field components, the FDTD equivalents of Maxwell's equations are then used to update the spatial distributions of these components at alternating half-time steps. The space steps are carefully chosen such that integral numbers of them can approximate the various dimensions of the structure. The super-absorbing first-order Mur boundary condition is utilized to terminate the FDTD lattice at the front and back planes in order to simulate infinite lines. On the other hand, the first-order Mur boundary condition is used on the other walls to simulate an open structure.

B. Experiment

In order to separate the effect of the connecting transmission lines on the discontinuities, the automatic network analyzer (HP8510C) is calibrated using a TRL calibration technique [12]. This technique relies on standards which are fabricated besides the discontinuities to be characterized on a single substrate. Fig. 2 shows a set of CPS TRL on-wafer standards which are used for calibrating the network analyzer. The standards consist of a CPS thru, a CPS short circuit and a CPS delay line. The calibration of the network analyzer is done using National Institute of Standards and Technology (NIST) de-embedding software program [13]–[15]. This program solves a 12-term error model from the thru line two-port measurements, the delay line two-port measurements and the two one-port reflection measurements. The program then establishes electrical reference planes to which all de-embedded S-parameters are referred. These planes are shown by dashed lines in Fig. 2. The reference impedance is set by the characteristic impedance Z_0 of the delay line.

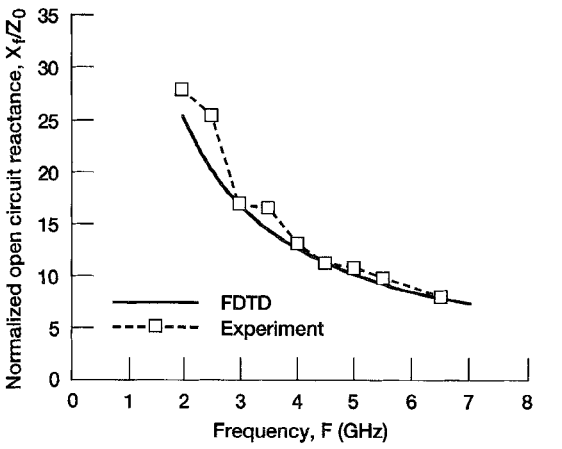

Fig. 4. Normalized open circuit reactance as a function of the frequency determined from the de-embedded reflection coefficient and the FDTD Model. $D = 0\,03$ in, $\epsilon_r = 10.2$, $W = 0.0285$ in, $S = 0.0055$ in and $Z_0 = 67\,5\ \Omega$.

III. CPS Open Circuit

A CPS open circuit is formed by abruptly ending the strip conductors as shown in Fig. 3. A fringing electric field exists at the open circuit between the two strip conductors and hence gives rise to a capacitive reactance. This capacitive reactance is modeled as a lumped capacitance C_f located at the plane $P - P'$. Fig. 4 presents the normalized open circuit reactance X_f/Z_0 as a function of the frequency F, for a fixed separation S. Fig. 4 also presents the normalized reactance obtained using the FDTD technique. The difference between the experimental and FDTD results can be attributed to the finite metal thickness which was not accounted for in the FDTD analysis. Specifically, in the FDTD method, zero thickness perfect electric conductors were assumed. It is worth mentioning that the circuit dimensions indicated in Fig. 4, and in all the subsequent figures are actual dimensions

TABLE I
OPEN END FRINGING CAPACITANCE C_f AS A FUNCTION OF THE SEPARATION S BETWEEN THE TWO STRIP CONDUCTORS AT A FIXED FREQUENCY $F = 3.5$ GHz, $D = 0.03$ IN, $\epsilon_r = 10.2$

Experimental W = 0.029 ± 0.0005 inch		FDTD Model W = 0.028			Quasi-Static [16] W = 0.028		
S (mils)	C_f (fF)	S (mils)	Z_0 (Ω)	C_f (fF)	S (mils)	Z_0(Ω)	C_f (fF)
5.5	42.5	5.6	68.8	45.76	5.6	68.8	30.8
7.8	43.4	7.5	74.3	45.23	7.5	74.3	28.7
9.05	40.1	9.3	79.0	44.87	9.3	79.0	28.2

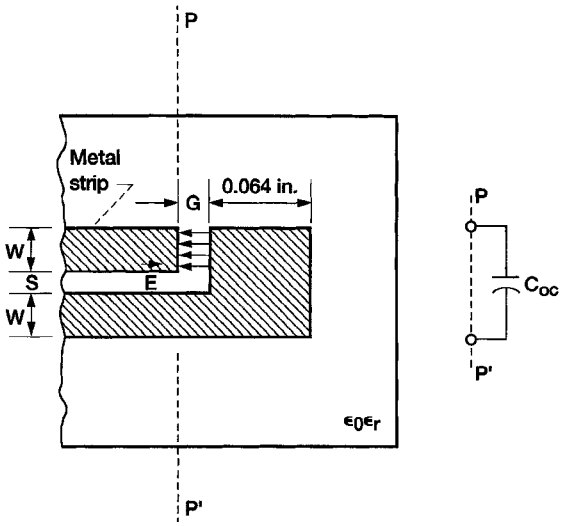

Fig. 5. Coplanar stripline open circuit with an extended strip conductor and a lumped capacitance equivalent circuit model.

TABLE II
OPEN CIRCUIT CAPACITANCE C_{oc} AS A FUNCTION OF THE GAP WIDTH G AT A FIXED FREQUENCY $F = 3.5$ GHz. $D = 0.03$ IN, $\epsilon_r = 10.2, W = 0.0282 \pm 0.0003$ IN, $S = 0.00575 \pm 0.00015$ IN

G (mils)	C_{oc}(pF)	
	Experimental	FDTD Model
6	0.1740	0.13
8.9	0.1709	0.118
12	0.1581	0.112

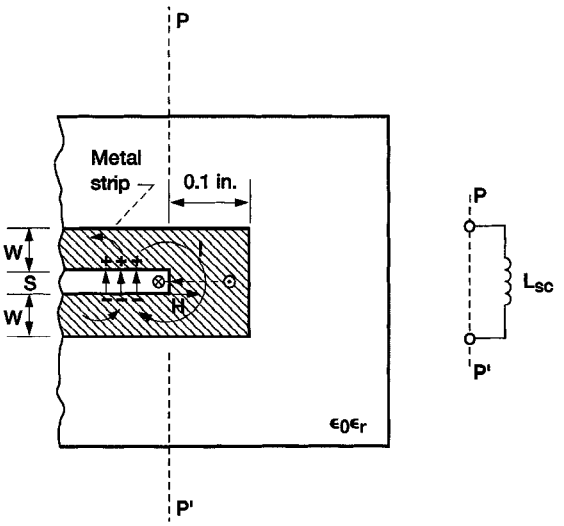

Fig. 6. Coplanar stripline short circuit and a lumped inductance equivalent circuit model.

after fabrication. However, the FDTD analysis considered dimensions slightly different from the actual dimensions due to the limitations in the used uniform discretization. Specifically for Fig. 4, the FDTD analysis considered a CPS open circuit with $S = 0.0056$ in and $W = 0.028$ in.

Table I shows the open end fringing capacitance C_f for three different separation distances S between the two strip conductors at a fixed frequency F. Also shown in Table I is the end capacitance obtained using the closed form expression derived in [16] which assumes a quasi-TEM mode of propagation on a CPS. The difference between the measured and FDTD results can be due to the reasons mentioned above. Also, for the CPS dimensions used, the quasi-TEM assumption is rather poor since the substrate thickness is equal to the strip width.

IV. CPS OPEN CIRCUIT WITH EXTENDED STRIP CONDUCTOR

A CPS open circuit with an extended strip conductor is shown in Fig. 5. In this case a gap of width G is formed at the open ends. An electric field exists across the gap G and hence gives rise to a capacitive reactance. This capacitive reactance is modeled as a lumped capacitance C_{oc} located at the plane $P - P'$. The capacitance C_{oc} is a parallel combination of the fringing and the gap capacitances. Table II shows the open end capacitance C_{oc} as a function of the open end gap width G at a fixed frequency F. From Tables I and II, the capacitance C_{oc} is about three to four times greater than the capacitance C_f. It is worth mentioning that the numerical de-embedding technique presented in [17] was used in conjunction with the FDTD technique to characterize the open end CPS discontinuities. Such a technique eliminates the need to use the CPS dispersion characteristics. Moreover the FDTD model used $S = 0.006$ in, $W = 0.028$ in and $Z_0 = 70\ \Omega$.

V. CPS SHORT CIRCUIT

A CPS short circuit is formed by filling the slot with a conductor as shown in Fig. 6. In this case a RF current flows

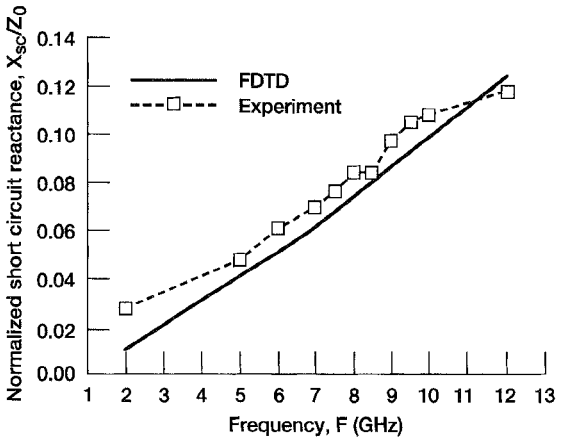

Fig. 7. Normalized short circuit reactance as a function of the frequency determined from the de-embedded reflection coefficient and the FDTD model. $D = 0.03$ in, $\epsilon_r = 10.2$, $W = 0.0285$ in, $S = 0.0056$ in and $Z_0 = 67.8\ \Omega$.

TABLE III
SHORT CIRCUIT INDUCTANCE L_{sc} AS A FUNCTION OF THE SEPARATION S BETWEEN THE TWO STRIP CONDUCTORS AT A FIXED FREQUENCY $F = 5.5$ GHz $D = 0.03$ IN, $\epsilon_r = 10.2$

Experimental W = 0.0288 ± 0.0003 inch		FDTD Model W = 0.028		
S (mils)	L_{sc}(pH)	S (mils)	Z_0 (Ω)	L_{sc}(pH)
4.5	70.95	4.0	63.4	76.8
5.9	80.46	6.0	70.0	93.3
7.8	108.95	8.0	75.6	110.2

around the end of the slot and hence there is magnetic energy stored behind the termination. This magnetic energy gives rise to an inductive reactance which is modeled as L_{sc} and located at the plane $P - P'$. Fig. 7 shows the variation of the normalized short circuit reactance X_{sc}/Z_0 as a function of the frequency F, for a fixed separation S. The small difference between the experimental and the FDTD modeled results is due to reasons similar to those mentioned earlier for an open circuit. The FDTD model considered a CPS short with $S = 0.0056$ in and $W = 0.028$ in. Table III shows the experimental and modeled short circuit inductance L_{sc} as a function of the separation S at a fixed frequency F.

VI. CPS Series Gap

A series gap of length G_1 in one of the strip conductors is shown in Fig. 8. The gap is modeled as a lumped Pi-network consisting of two fringing capacitances C_1 and a coupling capacitance C_2. Fig. 9 shows the de-embedded and FDTD modeled S parameters for the CPS series gap as a function of the frequency F. The FDTD model considers a CPS with $S = 0.0056$ in, $W = 0.028$ in, and a series gap with $G_1 = 0.00693$ in. Fig. 10 shows the variation of the experimentally obtained fringing and coupling capacitances, C_1 and C_2, as a function of the gap width G_1 at a fixed frequency F. As the gap width increases, the fringing capacitance increases and the coupling capacitance decreases.

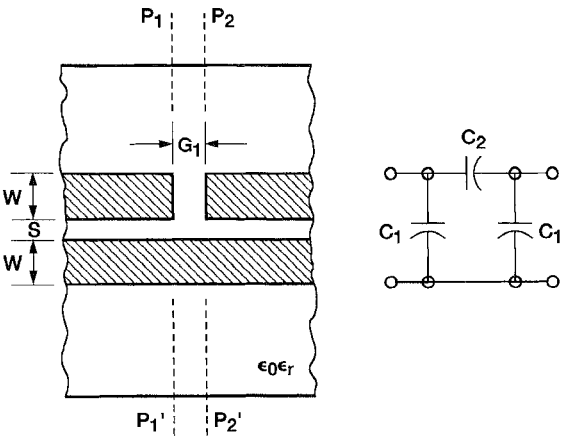

Fig. 8. Coplanar stripline series gap and a lumped pi-equivalent circuit model.

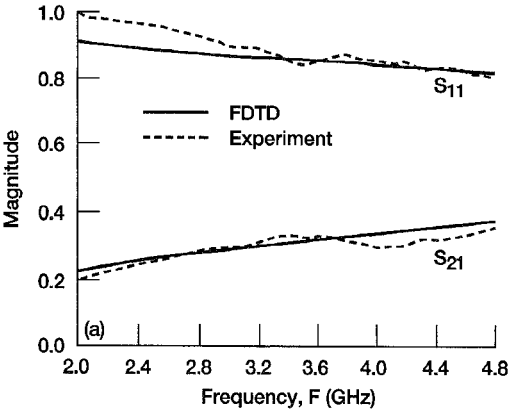

(a)

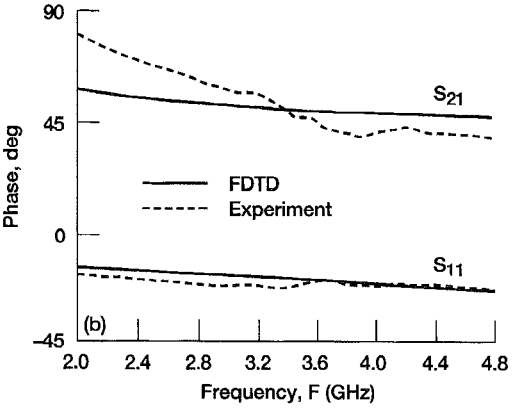

(b)

Fig. 9. Experimental and FDTD modeled S11 and S21 as a function of the frequency for the series gap. (a) Magnitude. (b) Phase. $D = 0.03$ in, $\epsilon_r = 10.2$, $W = 0.0284$ in, $S = 0.0056$ in and $G_1 = 0.0067$ in.

VII. CPS Spur-Slot and Spur-Strip

A CPS spur-slot and a CPS spur-strip structures are shown in Fig. 11. The spur-slot consists of a resonant structure created within the width of one of the strips. This structure is convenient to use when W is large and S is small. The spur-slot can be modeled as a short circuit stub of length $l \approx \lambda_{g(\mathrm{CPS})}/4$ in series with the main line. At resonance, the stub prevents the flow of RF power to the load. On the other

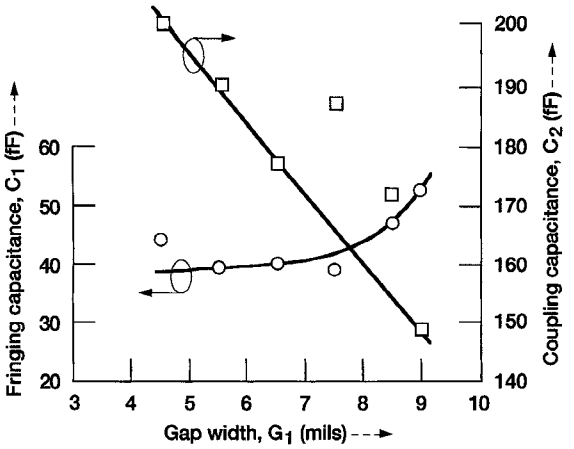

Fig. 10. Lumped fringing and coupling capacitances determined from the de-embedded measured S-parameters as a function of the gap width. $D = 0.03$ in, $\epsilon_r = 10.2, W = 0.0284$ in, $S = 0.0056$ in and $F = 4.025$ GHz.

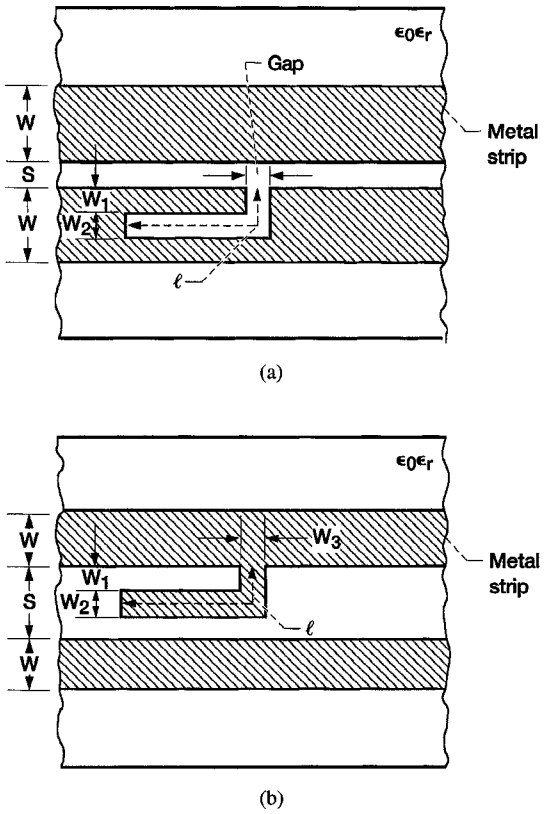

Fig. 11. Coplanar stripline with (a) spur-slot discontinuity. (b) Spur-strip discontinuity.

hand, the spur-strip consists of a resonant structure created between the two strip conductors. The spur-strip is convenient to use when W is small and S is large and can be modeled as a open circuit stub of length $l \approx \lambda_{g(\mathrm{CPS})}/4$ in parallel with the main line.

Fig. 12 shows the measured and FDTD modeled magnitude of the S-parameters, S_{11} and S_{21}, for a spur-slot as a function of the frequency F. The FDTD model considers a CPS with $S = 0.0075$ in, $W = 0.0275$ in and a spur-slot with $W_1 = 0.0075$ in, $W_2 = 0.0125$ in, Gap $= 0.0125$ in and $l = 0.645$

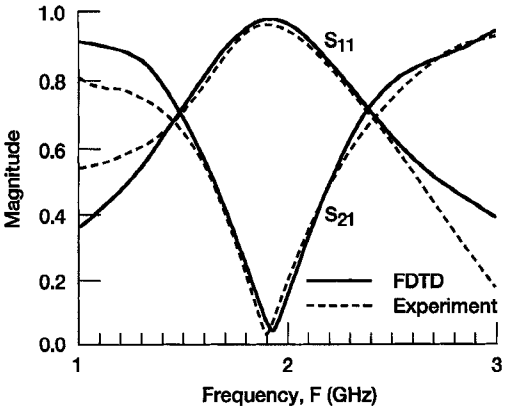

Fig. 12. Experimental and FDTD Modeled Magnitude of the S-parameters S_{11} and S_{21} as a function of frequency for a spur-slot. $D = 0.03$ in, $\epsilon_r = 10.2, W = 0.0275$ in, $S = 0.0075$ in, $W_1 = 0.0065$ in, $W_2 = 0.013$ in, Gap $= 0.013$ in and $l = 0.65$ in.

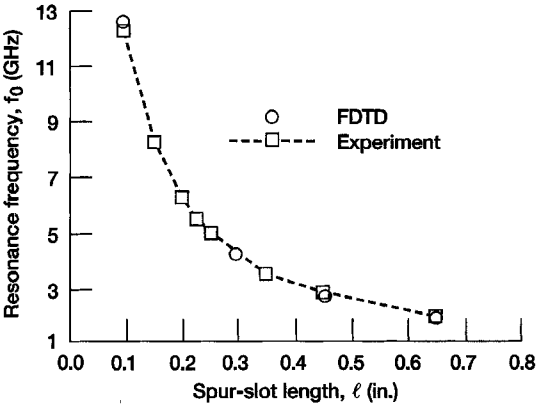

Fig. 13. Experimental and FDTD modeled resonance frequency as a function of the spur-slot length. $D = 0.03$ in, $\epsilon_r = 10.2, W = 0.0275$ in, $S = 0.0075$ in, $W_1 = 0.0065$ in, $W_2 = 0.013$ in, Gap $= 0.013$ in.

in. Fig. 13 shows the measured and FDTD modeled resonance frequency f_0 as a function of the spur-slot length l. The measured resonance frequency for the spur-strip is observed to be about the same as that of the spur-slot of equal length over the 2 to 12 GHz frequency range.

VIII. Conclusion

The paper presented for the very first time a measurement technique to obtain lumped equivalent circuit models for the following CPS discontinuities: an abrupt open circuit, an open circuit with an extended strip conductor, a short circuit, a series gap in one of the strip conductors and a spur-slot. The model element values are determined from the discontinuity S-parameters which are de-embedded from the measured S-parameters using a TRL algorithm. The model elements are presented as a function of the discontinuity physical dimensions for a specific substrate. The experimental results are compared to data obtained using the FDTD method and shown to be in good agreement. The measurement as well as the simulation techniques are quite general and can be extended to other substrate materials and higher frequencies. The CPS has potential applications in the design of microwave components such as filters, couplers, mixers, oscillators, and amplifiers for the emerging wireless communications.

REFERENCES

[1] J. B. Knorr and K. D. Kuchler, "Analysis of coupled slots and coplanar strips on dielectric substrate," *IEEE Trans. Microwave Theory Tech.*, vol. MTT-23, no. 7, pp. 541–548, July 1975.

[2] K. C. Gupta, R. Garg, and I. J. Bahl, *Microstrip Lines and Slotlines*. Dedham, MA: Artech, 1979, ch. 7 on Coplanar Lines, pp. 257–301.

[3] R. Goyal, Ed., *Monolithic Microwave Integrated Circuits: Technology & Design*. Norwood, MA: Artech House, 1989, ch. 4, sec. 4.7 on transmission lines, pp. 347–382.

[4] R. N. Simons, G. E. Ponchak, R. Q. Lee, and N. S. Fernandez, "Coplanar waveguide fed phased array antenna," in *Dig. 1990 IEEE Antennas Propagation Inter. Symp. URSI Radio Science Meet.*, vol. 4, pp. 1778–1781.

[5] R. N. Simons, N. I. Dib, R. Q. Lee, and L. P. B. Katehi, "Integrated uniplanar transition for linearly tapered slot antenna," *IEEE Trans. Antennas Propagat.*, vol. 43, no. 9, pp. 998–1002, Sept. 1995.

[6] T. Edwards, *Foundations for Microstrip Circuit Design*, 2nd ed.: Chichester, England: Wiley, 1992, ch. 5 and ch. 7, section 7.7 on microstrip resonator methods, pp. 245–261.

[7] R. N. Simons and G. E. Ponchak, "Modeling of some coplanar waveguide discontinuities," *IEEE Trans. Microwave Theory Tech.*, vol. 36, no. 12, pp. 1796–1803, Dec. 1988.

[8] K. S. Kunz and R. J. Luebbers, *The Finite Difference Time Domain Method for Electromagnetics*. Boca Raton, FL: CRC, 1993.

[9] X. Zhang and K. K. Mei, "Time-domain finite difference approach to the calculation of the frequency-dependent characteristics of microstrip discontinuities," *IEEE Trans. Microwave Theory Tech.*, vol. 36 , pp. 1775–1787, Dec. 1988.

[10] T. Shibata and H. Kimura, "Computer-aided engineering for microwave and millimeter-wave circuits using the FD-TD technique of field simulations," *Int. J. Microwave Millimeter-Wave Computer-Aided Eng.*, vol. 3, no. 3, pp. 238–250, May 1993.

[11] N. I. Dib, R. N. Simons, and L. P. B. Katehi, "New uniplanar transitions for circuit and antenna applications," *IEEE Trans. Microwave Theory Tech.*, vol. 43, no. 12, pp. 2868–2873, Dec. 1995.

[12] Hewlett Packard Product Note 8510-8A, Network Analysis: Applying the HP 8510 TRL calibration for noncoaxial measurements.

[13] NIST De-embedding Software, Program DEEMBED, Revision 4.04, 1994.

[14] G. F. Engen and C. A. Hoer, "Thru-Reflect-Line: An improved technique for calibrating the dual six-port automatic network analyzer," *IEEE Trans. Microwave Theory Tech.*, vol. MTT-27, no. 12, pp. 897–993, Dec. 1979.

[15] R. B. Marks, "A multiline method of network analyzer calibration," *IEEE Trans. Microwave Theory Tech.*, vol. 39, no. 7, pp. 1205–1215, July 1991.

[16] W. J. Getsinger, "End-effects in quasi-TEM transmission lines," *IEEE Trans. Microwave Theory Tech.*, vol. 41, pp. 666–672, Apr. 1993.

[17] Q. Chen and V. F. Fusco, "Numerical electromagnetic simulator termination de-embedding technique," *Electronics Lett.*, vol. 30, no. 5, pp. 423–424, Mar. 1994.

Rainee N. Simons (S'76–M'80–SM'89) received the B.S. degree in electronics and communications engineering from the Mysore University, India, in 1972, and the M.Tech. degree in electronics and communications engineering from the Indian Institute of Technology, Kharagpur, in 1974. In 1983 he received the Ph.D. degree in electrical engineering from the Indian Institute of Technology (IIT), New Delhi.

He started his career in 1979 as a Senior Scientific Officer at IIT, New Delhi. There he worked on finline components for mm-wave applications and also on X-Band toroidal latching ferrite phase shifters for phased arrays. From 1985 to present, he has been with the Space Electronics/Communications Division of NASA Lewis Research Center, Cleveland, OH, as a National Research Council Research Associate from 1985 to 1987, CWRU Research Associate from 1987 to 1990, Senior Engineer with Sverdrup Technology, Inc. from 1990 to 1993, and Senior Engineer with Nyma, Inc. from 1994 to present. At NASA LeRC he worked on optical control of MESFET and HEMT devices, high temperature superconductivity, modeling of coplanar waveguide (CPW) discontinuities, CPW feed systems for printed antennas, linearly tapered slot antenna arrays for communications and packaging of MMIC's. He is the author of a book entitled *Optical Control of Microwave Devices,* (Norwood, MA: Artech House). He has also authored a chapter entitled "High-Temperature Superconducting Coplanar Waveguide Microwave Circuits and Antennas" which has appeared in *Advances in High-Tc Superconductors* (Switzerland: Trans-Tech Publications.)

Dr. Simons has received the distinguished alumni award from his alma mater and several NASA Certificate of Recognition and Group Achievement awards. He organized a Special Session on "Advances in MMIC Packaging for Phased Array Antennas" at the 1993 IEEE AP-S International Symposium and URSI Radio Science Meeting. He served as a Guest Editor for the Special Issue on "Packaging Technologies for Phased Array Applications" published in the September 1995 issue of the IEEE TRANSACTIONS ON ANTENNAS AND PROPAGATION. He is a member of the Editorial Board of the IEEE TRANSACTIONS ON MICROWAVE THEORY AND TECHNIQUES.

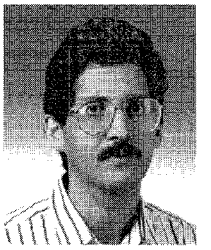

Nihad I. Dib (S'89–M'92) received the B.Sc. and M.Sc degrees in electrical engineering from Kuwait University in 1985 and 1987, respectively, and the Ph.D. degree in electrical engineering from the University of Michigan, Ann Arbor, in 1992.

From 1993 to 1995, he was an Assistant Research Scientist at the Radiation Laboratory at the University of Michigan. In 1995, he joined the Electrical Engineering Department at the Jordan University of Science and Technology as an Assistant Professor. His research interests include the numerical analysis and modeling of planar discontinuities and dielectric lines.

Linda P. B. Katehi (S'81–M'84–SM'89–F'95) received the B.S.E.E. degree from the National Technical University of Athens, Greece, in 1977, and the M.S.E.E. and Ph.D. degrees from the University of California, Los Angles, in 1981 and 1984, respectively.

In September 1984, she joined the faculty of the EECS Department, University of Michigan, Ann Arbor. She is currently a Professor of EECS. Her interest is in the development and characterization (theoretical and experimental) of microwave and mm-wave printed circuits, CAD of VLSI interconnects, micromachined circuits for mm-wave and submm-wave applications and low-loss lines for Terahertz applications. She has also been studying theoretically and experimentally various types of uniplanar radiating structures for hybrid-monolithic and monolithic oscillator and mixer designs.

Dr. Katehi has graduated 11 Ph.D. students and is presently supervising 15 Ph.D. graduate students. She has been the author and co-author of more than 220 papers published in referred journals and symposia proceedings. She was awarded the IEEE AP-S R.W.P. King (Best Paper Award for a Young Engineer) in 1984, the IEEE AP-S S.A. Schelkunoff Award (Best Paper Award) in 1985, the NSF Presidential Young Investigator Award and an URSI Young Scientist Fellowship in 1987, the Humboldt Research Award and the University of Michigan Faculty Recognition Award in 1994. She is a Fellow of the IEEE, and a Member of IEEE AP-S, MTT-S, Sigma XI, Hybrid Microelectronics, URSI Commission D and a Member of AP-S ADCOM from 1992 to 1995. She is also an Associate Editor for the IEEE TRANSACTIONS ON ANTENNAS AND PROPAGATION and IEEE TRANSACTIONS ON MICROWAVE THEORY AND TECHNIQUES.